

Flat bands with Berry curvature in multilayer graphene

Akshay Kumar¹ and Rahul Nandkishore^{2,*}

¹*Department of Physics, Princeton University, Princeton, NJ 08544, USA*

²*Princeton Center for Theoretical Science, Princeton University, Princeton, NJ 08544, USA*

(Dated: June 15, 2022)

We demonstrate that flat bands with local Berry curvature arise naturally in chiral (ABC) multilayer graphene placed on a boron nitride (BN) substrate. The degree of flatness can be tuned by varying the number of graphene layers N . For $N > 5$ the bands become nearly flat, with a small bandwidth $\sim 5\text{meV}$. The two nearly flat bands coming from the K and K' valleys cross along lines in the reduced zone. Weak intervalley tunneling turns the bandcrossing into an avoided crossing, producing two nearly flat bands with global Chern number zero, but with local Berry curvature. The flatness of the bands suggests that many body effects will dominate the physics, while the Berry curvature of the bands endows the system with a nontrivial quantum geometry. Multilayer graphene on BN thus provides a platform for investigating the interplay of interactions and quantum geometry which has no analog in the fractional quantum Hall effect. Flat bands with non-zero Chern number may also be realized by making use of magnetic adatoms, and explicitly breaking time reversal symmetry.

The behavior of strongly interacting electrons and the effect of quantum geometry are two of the most exciting fields of research in modern condensed matter physics. Strong interactions can give rise to effects such as fractionalization [1–3], where the elementary excitations carry some fraction of the ‘fundamental’ electronic quantum numbers, while a non-trivial quantum geometry [4] can lead to distinctive properties such as the existence of states that are protected against disorder [5, 6]. The two fields of research converge in the study of the fractional quantum Hall effect [7]. Recently, a strong interest has emerged in ‘fractional Chern systems:’ analogues of fractional quantum Hall systems where Berry curvature plays the role of magnetic field [8–17]. These systems allow us to study the interplay of strong correlations and quantum geometry in systems without magnetic field.

Fractional Chern physics arises in bands that are flat (non-dispersive) and Berry curved. The flatness of the bands means that interaction effects dominate over kinetic energy effects, allowing strong correlations to develop, while the non-vanishing Berry curvature endows the system with a non-trivial quantum geometry. Existing theory works have focused on flat bands where the integral of the Berry curvature over the zone is non-vanishing. These systems can be mapped onto fractional quantum Hall systems [13], and can be understood in terms of known fractional quantum Hall states. However, an exciting direction for future research involves flat bands with non-zero local Berry curvature, where the integrated Berry curvature vanishes. Such a bandstructure provides a platform for investigating the interplay of strong interactions and quantum geometry which has no analog in the fractional quantum Hall effect. However, the lack of material realizations of flat bands with Berry curvature represents a significant obstacle to advancement of this field.

In this letter, we show that flat bands with local

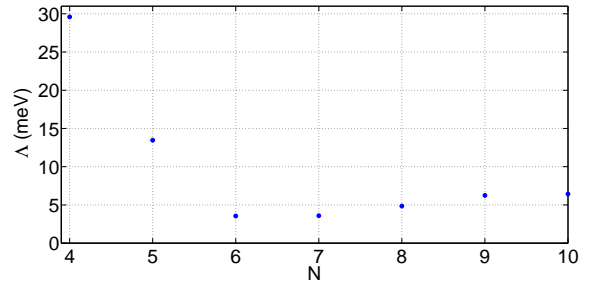


FIG. 1: Bandwidth Δ of the lowest conduction band for N layer chiral graphene. For $N > 5$, the bandwidth comes mainly from umklapp scattering at the zone boundary.

Berry curvature (but vanishing integrated Berry curvature) arise naturally in chiral multilayer graphene. Our proposal exploits the fact that ABC stacked multilayer graphene in the presence of a transverse electric field has a bandstructure with flat pockets that possess Berry curvature. Placing the graphene on a hexagonal Boron Nitride (BN) substrate then produces a superlattice potential such that the reduced Brillouin zone lies entirely within the flat pocket. Umklapp scattering opens a bandgap at the reduced zone edge. For a N layer system with $N > 5$ layers, the lowest band is nearly flat, with a bandwidth $\sim 5\text{meV}$. We have verified that this nearly flat band has a non-vanishing local Berry curvature. Chiral multilayer graphene thus provides an ideal platform for investigating the interplay of strong correlations and quantum geometry. Meanwhile, if a system with a direct analog in the fractional quantum Hall effect is desired, then flat bands with non-zero integrated Berry curvature may also be obtained via a more experimentally challenging setup, which uses magnetic adatoms rather than transverse electric field to open a gap between conduction and valence bands.

ABC stacked graphene: A single graphene sheet consists of a honeycomb lattice of carbon atoms. The honeycomb lattice consists of two sublattices, *A* and *B*. Chiral multilayer graphene consists of graphene sheets with an *ABC* stacking order (each succeeding sheet is rotated by $2\pi/3$ relative to the preceding sheet). Every lattice site in the bulk is either directly above or directly below another lattice site. In the $(\psi_{1A\mathbf{k}}\psi_{1B\mathbf{k}}\psi_{2A\mathbf{k}}\psi_{2B\mathbf{k}}\cdots\psi_{NA\mathbf{k}}\psi_{NB\mathbf{k}})$ basis, the nearest neighbor tight binding Hamiltonian for an N layer system takes the form [18]

$$H_0 = \begin{pmatrix} 0 & t_{\mathbf{p}} & 0 & 0 & 0 & 0 & \cdots \\ t_{\mathbf{p}}^* & 0 & \gamma & 0 & 0 & 0 & \cdots \\ 0 & \gamma & 0 & t_{\mathbf{p}} & 0 & 0 & \cdots \\ 0 & 0 & t_{\mathbf{p}}^* & 0 & \gamma & 0 & \cdots \\ 0 & 0 & 0 & \gamma & 0 & t_{\mathbf{p}} & \cdots \\ 0 & 0 & 0 & 0 & t_{\mathbf{p}}^* & 0 & \cdots \\ \vdots & \vdots & \vdots & \vdots & \vdots & \vdots & \ddots \end{pmatrix} \quad (1)$$

Here, $t_{\mathbf{p}} = t_0(\exp(ik_x a) + 2\exp(-i\frac{k_x a}{2})\cos(\frac{\sqrt{3}k_y a}{2}))$, represents nearest neighbor hopping within each graphene layer ($t_0 \approx 3eV$), and $\gamma \approx 300meV$ represents interlayer hopping between two sites that lie on top of each other. Here a is the lattice constant of graphene.

In the absence of interlayer hopping, $\gamma = 0$, the bandstructure consists of N copies of the graphene bandstructure, $E = \pm|t_{\mathbf{p}}|$ [19]. Near the two inequivalent corners of the Brillouin zone, conventionally labelled K and K' , the function $t_{\mathbf{p}}$ vanishes as $t_{\mathbf{p}} \approx v\mathbf{p}_+$ and $t_{\mathbf{p}} \approx -v\mathbf{p}_-$ respectively, where $\mathbf{p}_{\pm} = p_x \pm ip_y$ and $v = 3at_0/2$ is the Fermi velocity for graphene. Thus, there are two linear band-crossings at the two Dirac points, each of which is N fold degenerate. Each of the N bandcrossings carries a Berry phase of π (at the K point) or $-\pi$ (K' point).

We now consider interlayer hopping $\gamma \neq 0$. This interlayer hopping causes all the bulk sites to dimerize, opening up a bulk gap of size γ at the Dirac points. On the top and bottom surfaces, there are undimerized lattice sites, which give rise to gapless surface states. It is convenient to separate the low energy and high energy subspaces by writing the Hamiltonian in the $(\psi_{1A\mathbf{k}}\psi_{NB\mathbf{k}}\psi_{1B\mathbf{k}}\psi_{2A\mathbf{k}}\psi_{2B\mathbf{k}}\psi_{3A\mathbf{k}}\cdots\psi_{(N-1)B\mathbf{k}}\psi_{NA\mathbf{k}})$ basis. The Schrodinger equation in this basis becomes

$$\begin{pmatrix} H_{11} & H_{12} \\ H_{21} & H_{22} \end{pmatrix} \begin{pmatrix} \psi_{low} \\ \psi_{high} \end{pmatrix} = \varepsilon \begin{pmatrix} \psi_{low} \\ \psi_{high} \end{pmatrix}. \quad (2)$$

Here ε is the energy eigenvalue, ψ_{low} is a two component spinor, ψ_{high} is a $2N - 2$ component spinor, H_{11} is a 2×2 zero matrix and H_{12} and H_{22} are $2 \times (2N-2)$ and $(2N-2) \times (2N-2)$ matrices respectively. Here H_{12} and H_{22} have the form below

$$H_{12} = \begin{pmatrix} v\mathbf{p}_+ & 0 & \cdots & 0 & 0 \\ 0 & 0 & \cdots & 0 & v\mathbf{p}_- \end{pmatrix} \quad (3)$$

$$H_{22} = \begin{pmatrix} 0 & \gamma & 0 & 0 & 0 & \cdots \\ \gamma & 0 & v\mathbf{p}_+ & 0 & 0 & \cdots \\ 0 & v\mathbf{p}_- & 0 & \gamma & 0 & \cdots \\ 0 & 0 & \gamma & 0 & v\mathbf{p}_+ & \cdots \\ 0 & 0 & 0 & v\mathbf{p}_- & 0 & \cdots \\ \vdots & \vdots & \vdots & \vdots & \vdots & \ddots \end{pmatrix} \quad (4)$$

We can eliminate the high energy dimer components in the system of equations (2) to get a Schrodinger equation for only the low energy components in the manner of [20]. Since we are interested in only the low energy states, we make a binomial expansion to the first order in ε assuming it is very small compared to H_{22} . We get $(H_{eff} - \varepsilon)\psi_{low} = 0$ where $H_{eff} = (1 + H_{12}(H_{22})^{-2}H_{21})^{-1}(H_{11} - H_{12}(H_{22})^{-1}H_{21})$. This leads to a low energy single particle Hamiltonian for the surface states of an N layer graphene which takes the form

$$H_K(\mathbf{p}) = \frac{v^N}{(-\gamma)^{N-1}} \begin{pmatrix} 0 & p_+^N \\ p_-^N & 0 \end{pmatrix}; \quad p_{\pm} = p_x \pm ip_y \quad (5)$$

Here H_K is the Hamiltonian in the K valley, and the Hamiltonian in the K' valley is given by $H_{K'}(\mathbf{p}) = H_K^*(-\mathbf{p})$. We are using a basis such that $(1, 0)$ is a Bloch state in the *A* sublattice of the top layer, and $(0, 1)$ is a Bloch state in the *B* sublattice of the bottom layer. Only the lowest order terms have been written in each matrix element. This Hamiltonian is valid up to an energy scale γ . Note that this energy scale is independent of N , the number of layers of graphene. The above effective Hamiltonian consists of a single bandcrossing with non-trivial Berry phase $N\pi$, and low energy dispersion $E = \pm v^N p^N / \gamma^{N-1}$. Thus, the conduction band has a very flat pocket of a size $p \sim \gamma/v$ around the K and K' points, and this pocket becomes perfectly flat in the limit $N \rightarrow \infty$, corresponding to ‘rhombohedral graphite’.

Now consider the application of a transverse electric field leading to potential difference V between any 2 consecutive layers. We assume that $\gamma \gg e(N-1)V$. This ensures that the surface bands are much below the bulk bands. The low energy effective Hamiltonian then takes the form

$$H_K(\mathbf{p}) = \begin{pmatrix} \frac{\Delta}{2} & \frac{v^N}{(-\gamma)^{N-1}} p_+^N \\ \frac{v^N}{(-\gamma)^{N-1}} p_-^N & -\frac{\Delta}{2} \end{pmatrix} \quad (6)$$

The resulting band structure is plotted in Fig.2. We can see that a gap of magnitude $\Delta = (N-1)eV$ opens in the surface state spectrum. We can also see that the band near the K point is extremely flat, asymptoting to perfect flatness in the limit $N \rightarrow \infty$.

Effect of BN substrate: BN is a popular substrate for graphene. It has the same hexagonal structure, but with a slight lattice-mismatch (lattice constant $\sim \frac{56}{55}a$) and is a large band-gap insulator ($E_{gap} \sim 5eV$). Placing multilayer graphene on BN substrate introduces a superlattice

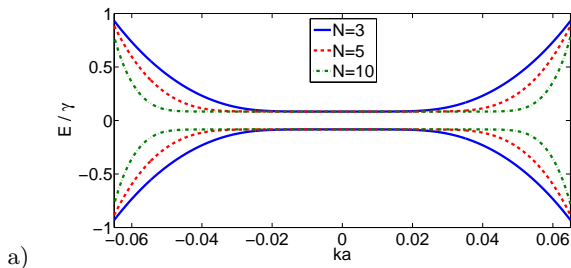


FIG. 2: Low energy band structure for N layer ABC stacked graphene in the presence of a transverse electric field. The band structure is plotted in the vicinity of the \mathbf{K} point, assuming that the potential difference between the top and bottom layers $\Delta = 0.167t_0 \approx 50meV$.

potential with a $Z \times Z$ supercell, where $Z = 56$. The primitive lattice vectors corresponding to the reciprocal lattice are

$$\begin{pmatrix} \mathbf{B}_1 \\ \mathbf{B}_2 \end{pmatrix} = \frac{2\pi}{3Za} \begin{pmatrix} 1 & \sqrt{3} \\ 1 & -\sqrt{3} \end{pmatrix} \begin{pmatrix} \hat{x} \\ \hat{y} \end{pmatrix} \quad (7)$$

The strong superlattice potential is seen primarily by states on the lower surface of the multilayer graphene, close to the substrate. These states are either conduction band or valence band states, depending on the sign of the transverse electric field. We assume the electric field is chosen such that it is the conduction band that mainly sees the superlattice potential. If the multilayer graphene were sandwiched between BN sheets, then both conduction and valence bands would see a strong superlattice potential, irrespective of the sign of electric field.

The reduced ‘Brillouin zone’ for the superlattice is hexagonal, but scaled by a factor $1/Z$ with respect to the original Brillouin zone. If Z is chosen such that $|\mathbf{K}|/Z < \gamma/v$, i.e. $Z > Z_c$, where

$$Z_c = 20\pi/\sqrt{3} = 36.3 \quad (8)$$

then the ‘flat pockets’ at K and K' extend over the entire reduced Brillouin zone. Moreover, umklapp scattering at the boundaries of the reduced Brillouin zone opens a gap between the flat pocket and the rest of the band. Since for BN substrate, $Z = 56 > Z_c$, it follows that placing chiral multilayer graphene on BN leads to flat bands that extend over the entire reduced Brillouin zone, and which are separated from the rest of the bandstructure by the umklapp energy scale λ .

We now explicitly calculate the bandstructure in the reduced zone. It may be readily determined that for the above superlattice potential, the K and K' points in the original zone get folded to inequivalent corners \tilde{K} and \tilde{K}' of the reduced zone. Meanwhile, the reciprocal lattice vectors of the superlattice satisfy $|\mathbf{B}_{1,2}| < \gamma/v < 2|\mathbf{B}_{1,2}|$, where γ/v is the width of the flat pocket. Since Bragg scattering is only effective between states that are near

degenerate, we restrict our attention to Bragg scattering by a single reciprocal lattice vector, and neglect higher order Bragg scattering events. The matrix elements of the superlattice potential $\langle \mathbf{k} | \hat{V} | \mathbf{k} + \mathbf{B}_{1,2} \rangle$ were determined by modelling the BN superlattice as a positive δ -function potential at each B site and a negative δ -function potential at each N site [23]. Hence we obtained the bandstructure in the reduced zone. Although the bandstructure contains $Z^2 = 56^2 = 3136$ conduction bands per spin and valley, only the lowest conduction band is flat, and is separated from the higher bands by an energy scale of order λ , where the gap may be estimated from the DFT calculations in [21], and is of order $10meV$. Meanwhile, the bandgap Δ between conduction and valence bands can be externally controlled using gates, and may be made as large as desired. We should take $\Delta \gg 10meV$ to ensure that we do not mix conduction and valence bands. For specificity, we suggest using $\Delta = 50meV$, which is easily achievable by gating [22].

From the bandstructure calculations, we can extract the bandwidth of the lowest conduction band. In Fig.1, we plot the bandwidth as a function of N . We see that for $N > 5$ the lowest conduction band is nearly flat, with a small residual bandwidth $\sim 5meV$ which comes mainly from umklapp scattering at the zone boundary. The $N = 6$ layer system actually has minimum bandwidth, due to a cancellation between ‘intrinsic’ curvature of the band and the effect of umklapp scattering.

We also note that there is an indirect band gap which vanishes for $N < 6$ and then decreases with increasing N . Transitions across the indirect band-gap must be phonon assisted and should be weak, but nevertheless it is essential that we work with $N > 5$ to have a truly isolated flat band. Fortunately, $N = 6$ is optimal not only through having the flattest band (Fig.1), but also because its indirect band gap is of order the direct band gap. For $N > 5$ the direct band gap is $\sim 5meV$.

We have now verified that the lowest conduction band can be made flat. Now we show that this band has non-vanishing Berry curvature. We calculate the Berry curvature of the band numerically by the method of non-Abelian Wilson loops [24]. This procedure proceeds as follows: we divide the reduced zone into plaquettes small enough such that the Chern flux through any plaquette is much less than 2π . The total flux is the sum of fluxes through all plaquettes. We calculate the flux through a particular plaquette by dividing its boundary into segments small enough that

$$\rho_{\mathbf{k},\delta} = \langle u_{\mathbf{k}} | u_{\mathbf{k}+\delta} \rangle \approx e^{i \int_0^\delta \langle u_{\mathbf{k}} | \partial_{\mathbf{k}} | u_{\mathbf{k}+\delta} \rangle} \quad (9)$$

where $|u_{\mathbf{k}}\rangle$ is a momentum eigenstate in the band of interest. The product of operators $\rho_{\mathbf{k},\delta}$ around the boundary of the plaquette gives the (exponentiated) line integral of the Berry phase, which is related to the Chern flux via Stokes’ theorem. The advantage of this non-Abelian

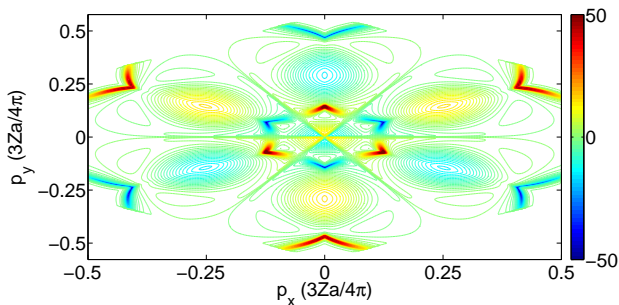


FIG. 3: Contour plot of Berry curvature in the lowest flat conduction band. The yellow regions come mainly from the K valley and have positive curvature, while the blue regions come mainly from the K' valley and have negative curvature. The Berry curvature integrated over the band is zero.

Wilson loop method is that it provides a way to calculate Chern fluxes by doing one dimensional integrals without requiring a smooth choice of gauge for the eigenstates [24]. It is thus well suited for numerical determination of Berry phases. It may be readily determined that the K and K' bands have opposite signs of local Berry curvature. Integrating over the reduced zone, we find the two valleys have integrated Berry curvature $\pm\pi$ respectively. However, the K and K' bands cross along lines in the reduced zone when we neglect intervalley tunneling.

The superlattice potential from the BN substrate introduces intervalley tunneling, of magnitude λ/Z [23], which turns the bandcrossings of K and K' bands into avoided crossings. The resulting bandstructure contains two strictly non-degenerate flat bands, separated by a minigap $\lambda/Z \approx 0.2meV$. The lowest energy band comes mostly from the K valley in regions closest to the \tilde{K} corner of the reduced zone, and comes mostly from the K' valley in regions closest to the \tilde{K}' corner. As a result, the lowest band contains regions with positive and negative local Berry curvature respectively (Fig.3). The integrated Berry curvature (Chern number) is zero.

Thus, we conclude that placing $N > 5$ layer ABC graphene on BN substrate allows us to realize two nearly flat bands with local Berry curvature, which are separated from the non-flat bands by a direct band gap of $5meV$ and are separated from each other by a minigap of $0.2meV$. ‘Quantum Hall ferromagnetism’ effects may lead to an exchange enhancement of the minigap, although this issue is beyond the scope of the present work. The principal outstanding theoretical problem consists of identifying experimentally detectable signatures of the interplay of interactions and quantum geometry in bandstructures with local Berry curvature, but zero Chern number. The novelty and experimental relevance of this problem make it highly desirable to investigate the effect of interactions in multilayer graphene.

Non-zero Chern number from adatoms. We close by noting that flat bands with non-zero Chern number may

be obtained by making use of adatom deposition to open a gap between conduction and valence bands, rather than using transverse electric field. An advantage of this method is that for the appropriate choice of (time reversal symmetry breaking) adatoms, the two valleys acquire the same sign of Berry curvature [25–27]. The rest of the analysis proceeds exactly as before, only now the Berry curvature has the same sign everywhere in the flat band, and thus does not cancel. However, adatom deposition represents a drastic change to the bandstructure, and cannot be dealt with easily using analytic techniques. Moreover, experimentally functionalization with adatoms is much more difficult than applying transverse electric field. An adatom functionalization of the form discussed in [25–27] has yet to be achieved successfully even for single layer graphene, whereas the application of transverse electric field to multilayer graphene samples is routine. Thus, we believe that applying transverse electric field to clean samples of multilayer graphene is the preferred route to flat bands with Berry curvature.

Concluding remarks. We have shown that ABC stacked multilayer graphene placed on BN substrate has a bandstructure containing flat bands. The six layer system is ideal for this purpose. The flat bands have nonzero local Berry curvature but zero Chern number, and thus have no analog in the fractional quantum Hall effect. Multilayer graphene thus presents an exciting new platform for investigating the interplay of interactions and quantum geometry in systems with zero Chern number. Bands with non-zero Chern number may also be produced using adatom deposition, however, this requires a further development of experimental techniques.

Acknowledgement We thank S.L.Sondhi for extensive discussions. We acknowledge useful conversations with E.J.Mele, L.S. Levitov, B.A.Bernevig, and L. Santos. A.K. is supported by NSF grant DMR-1006608.

* Electronic address: rahuln@princeton.edu

- [1] R. Rajaraman, arXiv:cond-mat/0103366 (unpublished).
- [2] R.B.Laughlin, Rev. Mod. Phys. 71, 863
- [3] J. Martin *et al*, Science 305 (5686): 9803 (2004)
- [4] F.D.M.Haldane, Phys. Rev. Lett. 107, 116801 (2011)
- [5] B. Blok and Xiao-Gang Wen. Nucl. Phys. B, 374:615 (1992).
- [6] M.Z.Hasan and C.L.Kane, Rev. Mod. Phys. 82, 3045
- [7] S.M.Girvin and A.H.MacDonald, in S.DasSarma and A.Pinczuk (Eds), *Perspectives in Quantum Hall Effects*, Wiley (1997).
- [8] E.Tang, J.-W. Mei and X.G.Wen, Phys. Rev. Lett. 106, 236802 (2011)
- [9] T. Neupert, L. Santos, C. Chamon and C. Mudry, Phys. Rev. Lett. 106, 236804 (2011)
- [10] K. Sun, Z.-C. Gu, H. Katsura and S. Das Sarma, Phys. Rev. Lett. 106, 236803 (2011)
- [11] N. Regnault and B. Andrei Bernevig, Phys. Rev. X 1,

- 021014 (2011)
- [12] Y.-L. Wu, B. Andrei Bernevig and N. Regnault, Phys. Rev. B 85, 075116 (2012)
- [13] S.A.Parameswaran, R. Roy and S. Sondhi, Phys. Rev. B 85, 241308(R) (2012)
- [14] G. Murthy and R. Shankar, <http://arxiv.org/abs/1108.5501>
- [15] R.-M.Lu and Y. Ran, Phys. Rev. B 85, 165134 (2012)
- [16] M. Trescher and E.J.Bergholtz, <http://arxiv.org/abs/1205.2245>
- [17] C.H.Lee, R. Thomale and X.-L. Qi, <http://arxiv.org/abs/1207.5587>
- [18] F. Zhang *et al*, Phys. Rev. Lett. 106, 156801 (2011)
- [19] P.R.Wallace, Phys. Rev. 71, 622634 (1947)
- [20] M. Koshino and E. McCann, Phys. Rev. B. 80, 165409 (2009)
- [21] B. Sachs, T.O.Webling, M.I.Katsnelson and A.I. Lichtenstein, Phys. Rev. B 84, 195414 (2011)
- [22] Y. Zhang *et al*, Nature, 459, 820-823 (Jun 2009)
- [23] See supplementary material.
- [24] Y.-L.Wu, N. Regnault and B. Andrei Bernevig, Phys. Rev. B 86, 085129 (2012)
- [25] Z. Qiao *et al*, Phys. Rev. B 82, 161414(R) (2010)
- [26] H. Zhang *et al*, Phys. Rev. Lett. 108, 056802 (2012)
- [27] J. Ding *et al*, Phys. Rev. B 84, 195444 (2011)

SUPPLEMENT

First, we calculate the matrix elements of the external potential \hat{V} coming from the BN between Bloch states, $\langle \mathbf{k} | \hat{V} | \mathbf{k} + \mathbf{q} \rangle$. This is just equivalent to calculating the Fourier transform of the BN potential. We model the BN potential as $\lambda' \delta(\mathbf{r}_i) - \lambda \delta(\mathbf{r}_j)$, where \mathbf{r}_i are the positions of boron atoms and \mathbf{r}_j are the positions of nitrogen atoms. This is a natural model, since the atomic numbers of *B* and *N* are one less than and one more than carbon respectively. Taking the delta functions to have slightly different weights will not qualitatively alter our results. The boron atoms sit on the A sublattice of the hexagonal superlattice, and the nitrogen atoms sit on the B sublattice.

The Fourier transform of the above potential takes the form

$$\langle \mathbf{k} | \hat{V} | \mathbf{k} + \mathbf{q} \rangle = \hat{V}(\mathbf{q}) = \delta_{\mathbf{k}, \mathbf{Q}} f_1(\mathbf{q}) \quad (10)$$

where \mathbf{Q} denotes a reciprocal lattice vector of the BN lattice (which is equal to $\mathbf{B}_{1,2}$ in Eq.7 of the main text modulo reciprocal lattice vectors of the graphene lattice) and $f_1(\mathbf{q})$ is a form factor coming from the two site nature of the BN unit cell. For the model potential under consideration, $f_1(\mathbf{q}) \propto (e^{i\mathbf{q} \cdot \mathbf{r}_i} - e^{i\mathbf{q} \cdot \mathbf{r}_j})$. Hence, we obtain $\langle \mathbf{k} | \hat{V} | \mathbf{k} + \mathbf{B}_1 \rangle = i\lambda$, $\langle \mathbf{k} | \hat{V} | \mathbf{k} + \mathbf{B}_2 \rangle = i\lambda$, $\langle \mathbf{k} | \hat{V} | \mathbf{k} + \mathbf{B}_1 + \mathbf{B}_2 \rangle = i\lambda$, and $f_1(-\mathbf{k}) = f_1^*(\mathbf{k})$.

Now, the band structure in the reduced Brillouin zone is found from the eigenvalues of the following 7×7 matrix:

$$\begin{pmatrix} m(\mathbf{k}, \mathbf{K}_0) & n^* & n & n & n & n^* & n^* \\ n & m(\mathbf{k}, \mathbf{K}_1) & n & 0 & 0 & 0 & n^* \\ n^* & n^* & m(\mathbf{k}, \mathbf{K}_2) & n & 0 & 0 & 0 \\ n^* & 0 & n^* & m(\mathbf{k}, \mathbf{K}_3) & n^* & 0 & 0 \\ n^* & 0 & 0 & n & m(\mathbf{k}, \mathbf{K}_4) & n^* & 0 \\ n & 0 & 0 & 0 & n & m(\mathbf{k}, \mathbf{K}_5) & n^* \\ n & n & 0 & 0 & 0 & n & m(\mathbf{k}, \mathbf{K}_6) \end{pmatrix} \quad (11)$$

where \mathbf{K}_0 points to the center of the central hexagon, $\mathbf{K}_1, \mathbf{K}_2, \mathbf{K}_3, \mathbf{K}_4, \mathbf{K}_5$ and \mathbf{K}_6 point to the centers of the 6 adjoining hexagons and

$$m(\mathbf{k}, \mathbf{Q}) = \begin{pmatrix} \Delta/2 & \frac{v^N ((k_x - Q'_x) - i((k_y - Q'_y)))^N}{(-\gamma)^{(N-1)}} & \frac{\lambda}{Z} & 0 \\ \frac{v^N ((k_x - Q'_x) + i((k_y - Q'_y)))^N}{(-\gamma)^{(N-1)}} & -\Delta/2 & 0 & \frac{\lambda}{Z} \\ \frac{\lambda}{Z} & 0 & \Delta/2 & \frac{v^N ((k_x - Q''_x) - i((k_y - Q''_y)))^N}{(-\gamma)^{(N-1)}} \\ 0 & \frac{\lambda}{Z} & \frac{v^N ((k_x - Q''_x) + i((k_y - Q''_y)))^N}{(-\gamma)^{(N-1)}} & -\Delta/2 \end{pmatrix} \quad (12)$$

$$n = \begin{pmatrix} i\lambda & 0 & 0 & 0 \\ 0 & i\lambda & 0 & 0 \\ 0 & 0 & i\lambda & 0 \\ 0 & 0 & 0 & i\lambda \end{pmatrix} \quad (13)$$

\mathbf{Q}' points to the *K* point of the hexagon whose center is given by \mathbf{Q} , for which the distance between \mathbf{k} and \mathbf{Q}' is the minimum. A similar definition holds for \mathbf{Q}'' and *K'* point.

Thus far we have assumed that the BN superlattice potential can be modelled as a delta function array. In fact, the B and N atoms carry + and - charge respectively. The BN superlattice potential may thus be better modelled as a delta function array convolved with a $1/r$ envelope. This Fourier transforms to a delta function array multiplied by a $1/k$ envelope. Thus intervalley scattering by Z reciprocal lattice vectors is weaker than intravalley scattering by one reciprocal lattice vector by a factor of $1/Z$. However, this weak intervalley scattering will still be important along lines in the reduced zone where the K and K' bands are degenerate.
